Available online at www.sciencedirect.com
SCIENCE DIRECT®
Journal of Power Sources 119–121 (2003) 805–810
JOURNAL OF POWER SOURCES
www.elsevier.com/locate/jpowsour

Thermal stability of lithium-ion battery electrolytes

Boris Ravdel[a,*], K.M. Abraham[a], Robert Gitzendanner[a], Joseph DiCarlo[a], Brett Lucht[b], Chris Campion[b]

[a]*Lithion Inc., 82 Mechanic St., Pawcatuck, CT 06379, USA*
[b]*University of Rhode Island, Department of Chemistry, Kingston, RI 02881, USA*

Abstract

The thermal decomposition of $LiPF_6$ in the solid state and as solutions in dialkylcarbonates has been investigated. The thermal decomposition of $LiPF_6$ was investigated with differential scanning calorimatry (DSC) suggesting decomposition to LiF and PF_5. In solution, PF_5 reacts with dialkylcarbonates to form a variety of decomposition products including carbon dioxide (CO_2), ethers (R_2O), alkylfluorides (RF), phosphorus oxyfluoride (OPF_3), and fluorophosphates (OPF_2OR, $OPF(OR)_2$). The structure of the decomposition products are supported by nuclear magnetic resonance (NMR) spectroscopy and gas chromatography with mass selective detection (GC–MS).

Keywords: Lithium-ion battery; Organic carbonate based electrolyte; Electrolyte decomposition

1. Introduction

Solutions of $LiPF_6$ in organic carbonate solvent mixtures are widely used as electrolytes in lithium-ion batteries. They are characterized by high conductivity, good electrochemical stability and the ability to perform at low temperatures. However, their thermal stability is poor even at moderately elevated temperatures of 60–85 °C. The salt is believed to play the role of a mediator in the solution's decomposition. A number of other salts have been tested as an alternative to $LiPF_6$ but they do not meet many of the requirements for the lithium-ion battery electrolytes (high conductivity, low cost, thermal stability, etc.). It would be useful to find a way to stabilize $LiPF_6$ solutions at high temperature. To achieve this goal the knowledge of the mechanism of the electrolyte decomposition is of great importance.

We have undertaken a detailed study of the thermal decomposition of $LiPF_6$ and its solutions in ethylene carbonate (EC), dimethylcarbonate (DMC), diethylcarbonate (DEC) and ethylmethylcarbonate (EMC), and mixed carbonates (up to 85 °C) with differential scanning calorimetry (DSC), conductivity, gas chromatography with mass selective detection (GC–MS), and nuclear magnetic resonance (NMR) spectroscopy. Preliminary results were recently reported [1]. The decomposition chemistry of $LiPF_6$ and its solutions in organic carbonates has been the focus of several recent studies [1–3], but many questions remain unsolved. Our analysis of the decomposition of $LiPF_6$/carbonate electrolytes has primarily focused on two areas: the thermal decomposition of solid $LiPF_6$ and that of $LiPF_6$ solutions of EMC, DMC, and DEC.

2. Experimental

Battery grade carbonate solvents obtained from EM Industries were used without further purification. Battery grade $LiPF_6$ obtained from Hashimoto Chemical Corporation, Tomiyama High Purity Chemicals, or Advance Research Chemicals Inc., was used without further purification.

The conductivity was measured with a Metrohm 712 conductivity meter using Orion 018010 or Metrohm AG 9101 conductivity cells (the cell constant was 1 cm^{-1} for each cell). The conductivity cell was enclosed in an airtight Ace Glass-Thred glass jacket by means of Ace-Thred Teflon adapter and a FETFE O-ring. The cell contained 6–7 ml of the solution. This design of the conductivity cell allows conductivity measurements to be conducted outside the glove box (Vacuum Atmosphere Glove Box, moisture content below 1 ppm) without atmospheric contamination. The temperature of the conductivity cell was maintained at

* Corresponding author. Tel.: +1-860-599-1100x467; fax: +1-860-599-5122.
E-mail address: bravdel@lithion.com (B. Ravdel).

0378-7753/03/$ – see front matter
doi:10.1016/S0378-7753(03)00257-X

±0.1 °C by means of a Tenney Environmental chamber. Solutions for storage studies were sealed in ampoules and stored in an oven. The glass ampoules were filled in the glove box and evacuated to a pressure of approximately 1 mmHg before hermetically sealing them. After the thermal treatment at the desired temperature, the ampoules were opened in the argon filled glove box and the solution was transferred into the conductivity cell. In addition, in situ conductivity measurements were performed on solutions in a conductivity cell, which was heated and the conductivity was monitored as a function of time.

Differential scanning calorimetry measurements were performed on TA Instruments 2010 DSC. Typically, 10 mg of the sample was sealed into a hermetic aluminum pan in the argon filled glove box. The pan was placed in the DSC cell, which was cooled to −150 °C with liquid nitrogen. Thermograms were obtained at scan rates varying from 2 to 10 °C/min.

Samples for gas chromatography with mass selective detection or nuclear magnetic resonance spectroscopy were prepared in the argon filled gloved box followed by flame sealing in ampoules or NMR tubes. Additional investigations were carried out utilizing Teflon valved NMR samples. Samples were heated at 85 °C for extended times. NMR analyses were conducted on a JEOL 400 MHz NMR spectrometer. ^{19}F NMR resonances are referenced to $LiPF_6$ at 65.0 ppm and ^{31}P NMR spectra were acquired with broadband ^{1}H decoupling and are referenced to $LiPF_6$ at −145.0 ppm. GC–MS analyses were conducted on an Agilent Technologies 6890 GC with a 5973 mass selective detector and a HP-5MS column. Helium was used as the carrier gas with a flow rate of 3.3 ml/min. Gaseous samples were ramped from 50 to 100 °C at 5.5 °C/min. Liquid samples were first ramped from 30 to 50 °C at 5 °C/min followed by ramping at 10 °C/min to 250 °C.

3. Results

3.1. Investigations of solid $LiPF_6$

The DSC thermograms of solid $LiPF_6$ were dependent upon experimental conditions. $LiPF_6$ in sealed pans reveals a sharp reversible endothermic peak at 193.7 ± 0.3 °C with a heat input of 1.93 ± 0.04 kJ/mol (Fig. 1, curve 1). The pans remained hermetic after the scanning, and when the same sample was tested again, the result was the same as in the first scan. This peak does not appear to be a melting point because we could not observe fusing when the salt was heated in a sealed glass capillary up to 220 °C. Being reversible, the peak may correspond to a solid-phase transformation.

The picture is quite different in an open pan with flowing argon. When the sample pan was isothermally heated in high purity flowing argon (Airco, Grade 5, 99.999%, moisture content 1 ppm) at about 85 °C, 25–30% weight loss was observed during a period of 10 h, indicating slow decomposition of the salt. The process is too slow to observe any heat flow in the DSC below 150 °C. Upon scanning, an endothermic decomposition with an onset temperature of 150–160 °C and a peak temperature of about 225 °C appears (Fig. 1, curve 2). The peak at 193 °C is still present, overlapping with the decomposition peak.

The endothermic nature of $LiPF_6$ decomposition and its dependence on sample pressure (open pan versus closed pan) are in agreement with the equilibrium in Eq. (1) [5].

$$LiPF_6(s) \Leftrightarrow LiF(s) + PF_5(g) \quad (1)$$

This is confirmed by weight measurements of the sample in open pan after prolonged heating.

In flowing argon containing trace amounts of moisture (Airco, high pressure, unspecified impurities content

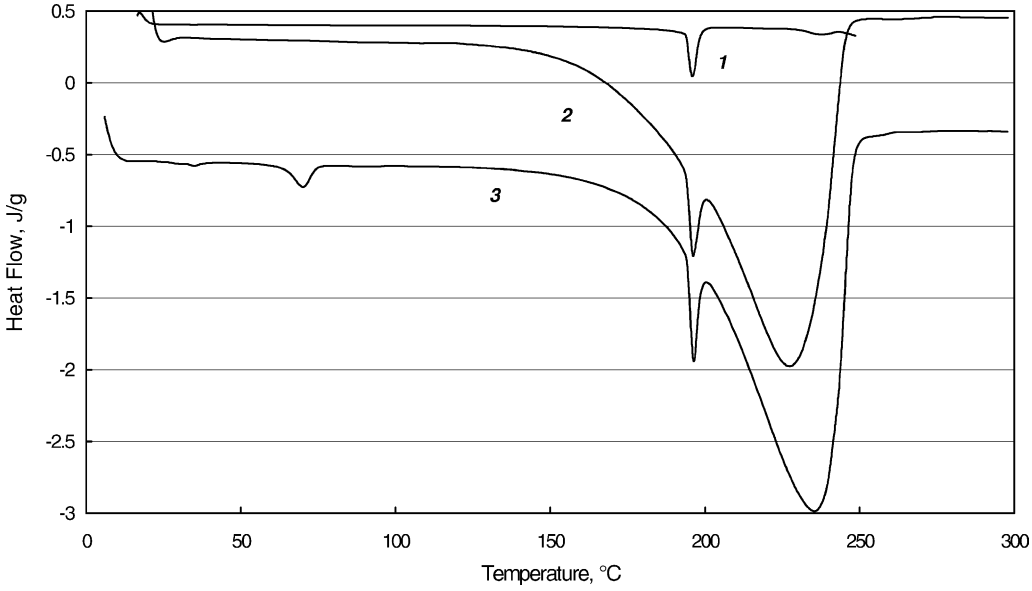

Fig. 1. DSC thermograms for $LiPF_6$. (1) Sealed pan; (2) open pan with high purity argon flow; (3) open pan with low purity argon.

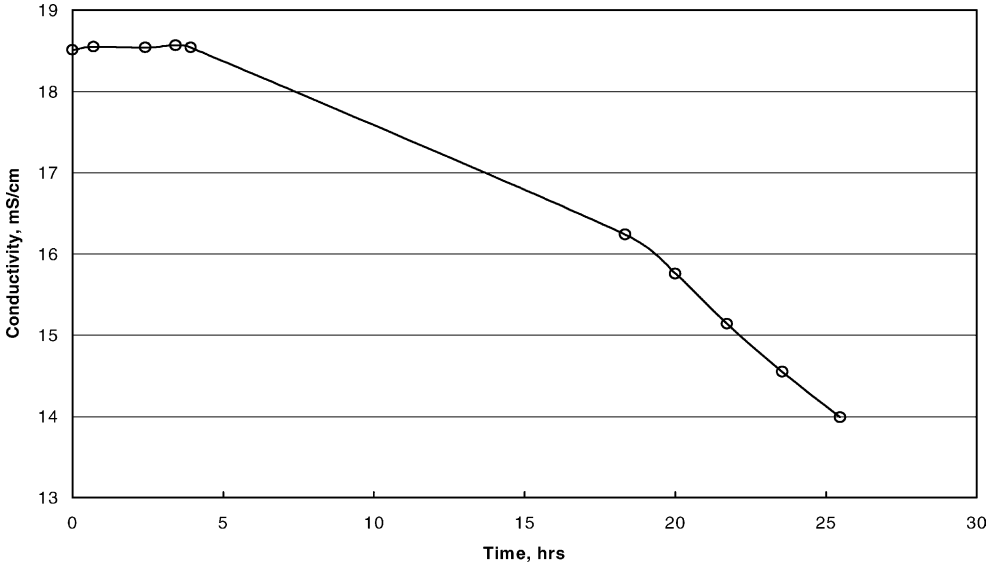

Fig. 2. Conductivity of 1.0 M $LiPF_6$ in EC:DMC:DEC (1:1:1) stored at 85 °C.

20 ppm), an additional endothermic peak appears at about 60 °C (Fig. 1, curve 3). Its heat input varied from 1 to 15 J/g depending on the scan rate. We ascribe this peak to the formation of phosphorus oxyfluoride (OPF_3) from reaction of $LiPF_6$ with water as described in Eq. (2).

$$LiPF_6(s) + H_2O(g) \rightarrow LiF(s) + OPF_3(g) + 2HF(g) \quad (2)$$

In electrolyte solutions, it is most likely that PF_5 and OPF_3 initiate solvent decomposition forming a number of liquid and gaseous products as described below.

3.2. Investigation of $LiPF_6$ in carbonate solutions

All of the solutions investigated reveal visible changes upon heating. First, the solutions become colored, and then precipitate appears. The visual changes are accompanied by changes in conductivity and spectroscopic properties. The rate of the decomposition depends on temperature and the structure of the carbonate. Decomposition is detected upon heating samples above 70 °C over 2–3 days, but occurs more rapidly when samples are stored at 85 °C.

3.3. $LiPF_6$ in 1:1:1 ethylene carbonate (EC):dimethyl carbonate (DMC):diethyl carbonate (DEC)

The conductivity of 1.0 M $LiPF_6$ in 1:1:1 EC:DMC:DEC decreases by approximately 25% during the first 26 h of storage at 85 °C (Fig. 2). This dramatic loss of conductivity prompted further investigation of electrolyte decomposition products. The liquid electrolytes were investigated by multinuclear NMR spectroscopy. The spectroscopic results confirm electrolyte decomposition. Upon heating samples containing 1.0 M $LiPF_6$ in EC:DMC:DEC at 85 °C, we observed solution graying after 48 h followed by continued darkening and precipitation of black solids upon heating for 1 week (168 h). ^{1}H NMR spectra of samples heated for 168 h at 85 °C reveal many new resonances characteristic of electrolyte decomposition (Fig. 3). Related new resonances characteristic of decomposition were also observed by ^{19}F and ^{31}P NMR spectroscopy. However, due to the complexity of the spectral data we were unable to characterize all of the

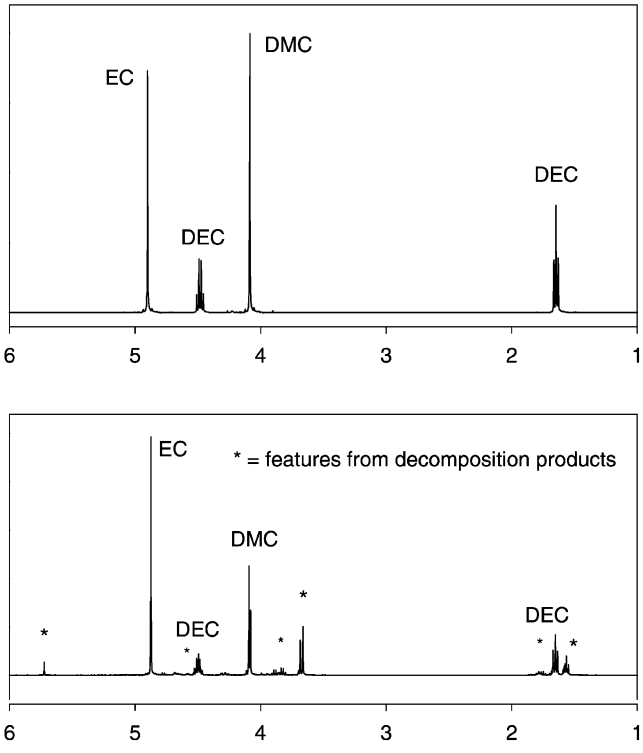

Fig. 3. Top: ^{1}H NMR spectrum of 1.0 M $LiPF_6$ in 1:1:1 EC:DMC:DEC before heating; bottom: ^{1}H NMR spectrum of 1.0 M $LiPF_6$ in 1:1:1 EC:DMC:DEC after heating for 1 week (160 h).

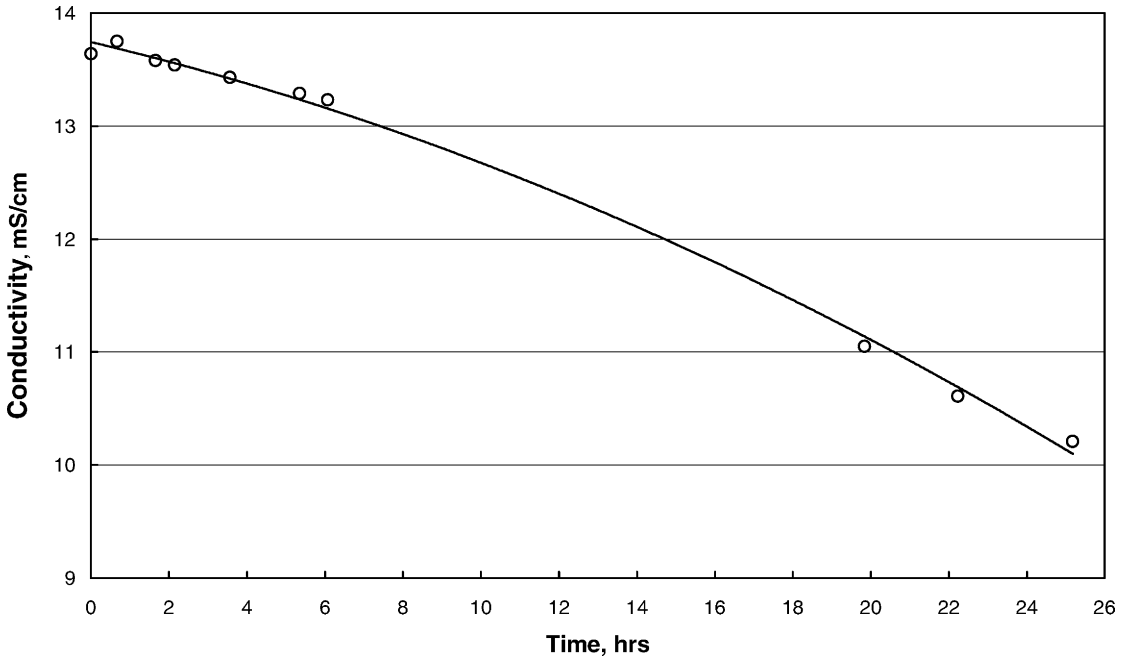

Fig. 4. Conductivity of 1.0 M $LiPF_6$ in DMC stored at 84 °C.

decomposition products. In order to simplify the characterization of decomposition products, we investigated the thermal decomposition of $LiPF_6$ dissolved in single carbonates. The decomposition of DMC, DEC, and EMC are discussed below. Efforts to characterize the decomposition products of 1.0 M $LiPF_6$ in EC have proven difficult and will be reported in due time.

3.4. $LiPF_6$ in dimethyl carbonate (DMC)

While samples of 1.0 M $LiPF_6$ in DMC show a significant decrease in conductivity after storage at 84 °C for 26 h (Fig. 4), the decrease is less than that described above for the mixed carbonate system. We also observe significantly less solid precipitate in samples consistent with a lack of oligomeric and polymeric carbonates that have been observed in thermally decomposed electrolytes containing EC [4].

Samples of 1.0 M $LiPF_6$ in DMC heated at 85 °C for 500 h turned a light shade of gray with trace white precipitate. Analysis of the decomposed solution was conducted with a combination of GC–MS and multi-nuclear NMR spectroscopy. The vapor phase of 1.0 M $LiPF_6$ in DMC samples contained several peaks on the gas chromatogram. The first peak is consistent with a mixture of carbon dioxide (CO_2), and OPF_3 as determined by spectral matching against the National Institute of Standards (NIST) library. The second peak is consistent with dimethylcarbonate. Analysis of the vacuum transferred liquid phase contains small peaks consistent with PF_5 (0.73 min), dimethylether (0.75 min), and $OPF_2(OCH_3)$ (0.84 min) (Fig. 5). The first two peaks match against the NIST library while the third peak has a fragmentation pattern consistent with $OPF_2(OCH_3)$ (m/z = 116, 115, 97, 87, 86, 85, 69, 47, 31, 29). $OPF_2(OCH_3)$ is not included in the NIST library. The chromatogram also includes a very large peak characteristic of dimethylcarbonate (0.96 min) along with several other small peaks that remain uncharacterized.

NMR spectra of 1.0 M $LiPF_6$ in DMC provide additional information on the structure of the decomposition products. All samples contain ^{19}F and ^{31}P NMR resonances characteristic of $LiPF_6$. Samples containing $LiPF_6$ and DMC heated at 85 °C for 500 h contain additional NMR resonances. Both ^{19}F and ^{31}P NMR spectra contain one primary new resonance. ^{19}F NMR spectra contain a new doublet (51.1 ppm, J_{P-F} = 1005) while ^{31}P NMR spectra feature a new triplet (−20.5 ppm, J_{P-F} = 1006). This coupling pattern is consistent with a single phosphorus atom directly bound to two fluorine atoms as would be expected for

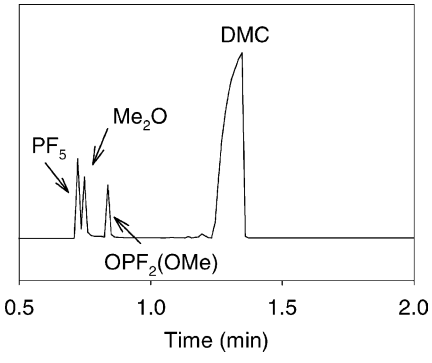

Fig. 5. Gas chromatogram of liquid phase of 1.0 M $LiPF_6$ in DMC heated at 85 °C for 500 h after vacuum transfer.

$OPF_2(OCH_3)$. Additional small resonances are observed in both ^{19}F and ^{31}P NMR spectra but remain uncharacterized. We do not observe resonances characteristic of OPF_3 or PF_5.

3.5. $LiPF_6$ in diethyl carbonate (DEC)

Analyses of samples containing 1.0 M $LiPF_6$ in DEC provide similar results to those observed for DMC. Samples turned a light shade of gray after heating at 85 °C for 65 h. Continued heating resulted in increased darkening and the formation of white precipitate. GC–MS analysis of the vapor phase of samples containing 1.0 M $LiPF_6$ in DEC contain a large peak corresponding to a mixture of gasses similar to those reported for dimethylcarbonate and include CO_2 and OPF_3 as determined by matching against the NIST library. The vacuum transferred liquid phase of 1.0 M $LiPF_6$ in DEC includes peaks representative of PF_5, fluoroethane, diethylether, OPF_3, and a large broad peak corresponding to DEC. Other peaks in the chromatogram have mass spectra supporting $OPF_2(OEt)$ and $OPF(OEt)_2$. The second compound matches to the NIST library while the first compound has fragmentation pattern consistent with $OPF_2(OEt)$ (m/z = 129, 115, 103, 85, 69, 45) but is not included in the NIST library. The parent ion (m/z = 130) is not observed but the base peak corresponds to M–C_2H_3 which is an intense fragment for both $OPF(OEt)_2$ and $OP(OEt)_3$. In addition, we observe several uncharacterized peaks in the gas chromatogram.

NMR spectra of samples containing 1.0 M $LiPF_6$ in DEC provide additional support for the species observed by GC–MS. Spectra were acquired at regular time intervals during the course of the thermal decomposition and support the formation of many new compounds. Three of these compounds have been characterized. The first new resonances observed upon heating the sample at 85 °C for 140 h are characteristic of $OPF_2(OEt)$ (**1**) and fluoroethane. Compound **1** displays a ^{19}F doublet (53.7 ppm, J_{P-F} = 1003) and a ^{31}P triplet (−21.2 ppm, J_{P-F} = 1005) while fluoroethane displays a ^{19}F triplet of quintets (−73.1 ppm, J_{H-F} = 47.2, 26.1). With continued heating (500 h) the resonances characteristic of **1** and EtF increase in intensity and additional resonances characteristic of $OPF(OEt)_2$ (**2**) are observed (^{19}F doublet; 56.4 ppm, J_{P-F} = 959, ^{31}P doublet; −11.2 ppm, J_{P-F} = 961) (Fig. 6). Additional small resonances are observed in both the ^{19}F and ^{31}P NMR spectra but remain uncharacterized. ^1H NMR spectra contain additional support of the proposed decomposition products. Resonances characteristic of diethylether are observed at 3.65 and 1.28 ppm while resonances consistent with **1** and **2** [4.66 (mult), 4.47 (mult), 1.57 (t, 6.8), 1.50 (t, 7.0)] are observed.

3.6. $LiPF_6$ in ethylmethyl carbonate (EMC)

Analyses of samples containing 1.0 M $LiPF_6$ in EMC provide similar results to those described for $LiPF_6$ in DMC and DEC. GC–MS analysis of samples stored at 85 °C for 500 h reveal the presence of CO_2, Me_2O, Et_2O, EtOMe, EtF, OPF_3, DMC, and DEC. The concentrations of DMC and DEC are much higher than the decomposition products suggesting that the ester exchange reactions of alkyl carbonates are more facile than the decomposition reactions. The high rate of ester exchange in dialkylcarbonates was confirmed by ^1H NMR spectroscopic investigations. Ester exchange will be discussed below in the context of the mechanism of electrolyte decomposition.

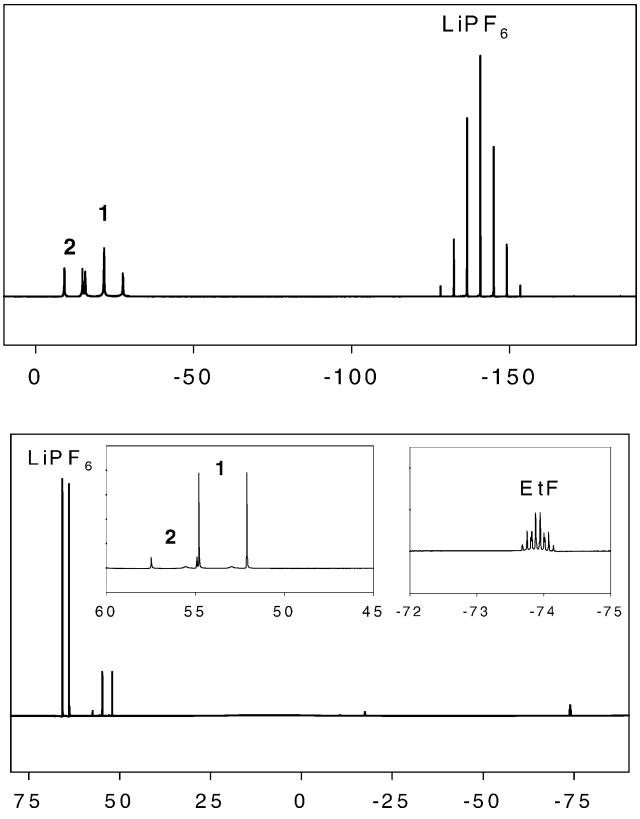

Fig. 6. Top: ^{31}P NMR spectrum of 1.0 M $LiPF_6$ in DEC after heating at 85 °C for 500 h; bottom: ^{19}F NMR spectrum of 1.0 M $LiPF_6$ in DEC after heating at 85 °C for 500 h. Insets include expanded regions of spectrum.

4. Discussion

The thermal decomposition of $LiPF_6$ in dialkylcarbonates provides a range of decomposition products summarized in Table 1. We have not conducted a thorough mechanistic

Table 1
Summary of decomposition products observed by GC–MS and multinuclear NMR spectroscopy

Carbonate	Observed products
DMC-$LiPF_6$	PF_5, OPF_3, CO_2, Me_2O, $OP(OMe)F_2$
DEC-$LiPF_6$	PF_5, OPF_3, CO_2, Et_2O, EtF, $OP(OEt)F_2$, $OP(OEt)_2F$
EMC-$LiPF_6$	PF_5, OPF_3, CO_2, Me_2O, EtOMe, Et_2O, EtF, EMC, DMC, $OP(OEt)F_2$

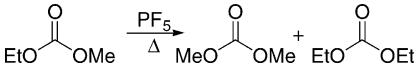

Scheme 1.

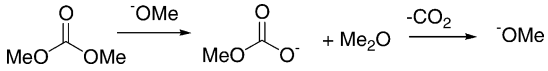

Scheme 3.

investigation of the thermal decomposition, but the observed products can be generated via well-known reaction mechanisms. The thermal decomposition of $LiPF_6$ to LiF and PF_5 has been described elsewhere [5] and has been confirmed in our DSC experiments on solid $LiPF_6$. The rearrangement of carbonates via Lewis acid mediated ester exchange reactions is displayed in Scheme 1. The rapid ester exchange reaction suggests transient formation of alkoxide anions.

The alkoxide displacent of fluoride in PF_5 produces $ROPF_4$. Further addition of alkoxide anions to the same P(V) center can provide $(RO)_2PF_3$ and $(RO)_3PF_2$. It is well known that P(V) compounds containing at least one alkoxide and one halide substituent are susceptible to Arbuzov rearrangements [6]. Rearrangements of $ROPF_4$, $(RO)_2PF_3$ and $(RO)_3PF_2$ produce OPF_3, $OPF_2(OR)$, and $OPF(OR)_2$, respectively (Scheme 2) along with one equivalent of alkylfluoride (RF). The thermal decomposition of $LiPF_6$ in DEC results in the formation of ethylfluoride along with $OPF_2(OR)$ and $OPF(OR)_2$ supporting the mechanistic hypothesis. However, we do not observe evidence of methylfluoride in DMC solutions of $LiPF_6$. Since the thermal decomposition of $LiPF_6$ in DMC is slower than the corresponding decomposition in DEC during the timescale of our experiments a very low concentration of methylfluoride would be expected. We suspect that the mechanisms are similar and the methylfluoride is eluding our detection. The thermal decomposition of DEC in the presence of PF_6 is significantly more rapid that that of DMC. This is expected for decomposition mechanisms related to the Arbuzov rearrangement. The transition state for elimination of alkylfluoride in Arbuzov rearrangements involves a nucleophilic attack of fluoride on the α-carbon of alkoxy substituents. Nucleophilic attacks are favored on primary carbons over methyl carbons. This reaction mechanism is related to those proposed for the reaction of PF_5 with dimethylether [7] and the Lewis acid catalyzed polymerization of cyclocarbonates [8].

The generation of the decomposition products diethyl and dimethylether can be generated via alkyl–oxygen cleavage reactions, which frequently accompany transesterification reactions (Scheme 3) [9]. This reaction is particularly detrimental since upon ether formation the carbonate anion

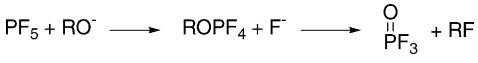

Scheme 2.

decarbonolates generating CO_2 and regenerating an equivalent of methoxide for further decomposition reactions (Scheme 3).

5. Conclusions

The thermal decomposition of $LiPF_6$ in carbonates has been investigated by a combination of DSC, conductivity, GC–MS, and NMR spectroscopy. The observed decrease in ionic conductivity of 1.0 M $LiPF_6$ dialkylcarbonate solutions correlates with electrolyte decomposition observed by GC–MS and multi-nuclear NMR spectroscopy. These mechanistic hypotheses suggest that preventing transesterification of dialkylcarbonates should inhibit thermal decomposition of $LiPF_6$/carbonate based electrolytes. Preliminary investigations suggest that addition of appropriate additives can increase the thermal stability of $LiPF_6$ in carbonate solvents by two-orders of magnitude. We will report these results in due course.

Acknowledgements

We would like to thank the United States Air Force for financial support of this research under contract No. 33615-98-C-2898.

References

[1] B. Ravdel, K.M. Abraham, R. Gitzendanner, C. Marsh, in: Proceedings of the 200th Meeting of the ECS, San Francisco, 2–7 September 2001, Meeting Abstracts, p. 97.
[2] S.K. Singh, P.J. Ralbovsky, G.A. Melhem. Pittcon, Abstracts, New Orleans, 4–9 March 2001, p. 809.
[3] G.G. Botte, R.E. White, Z. Zhang, J. Power Sources 97–98 (2001) 570.
[4] S.E. Sloop, J.B. Kerr, K. Kinoshita, Electrochem. Solid-State Lett. 4 (2001) A42.
[5] N.N. Greenwood, A. Earnshaw, Chemistry of the Elements, Pergamon Press, New York, 1997, pp 498–499.
[6] G.M. Kosolapoff, Organophosphorus Compounds, Wiley, New York, 1950, pp. 213–214.
[7] R.A. Goodrich, P.M. Treichel, J. Am. Chem. Soc. 88 (1966) 3509.
[8] H.R. Kircheldorf, B. Weegen-Schlz, Makromol. Chem., Rapid Commun. 14 (1993) 405.
[9] J. March, Advanced Organic Chemistry, 3rd ed., Wiley, New York, 1985, p 351.